

## 4 $\pi$ DETECTORS\*

G. J. FELDMAN

Stanford Linear Accelerator Center, Stanford University, Stanford, California 94305

M. G. D. GILCHRIESE

Cornell University, Ithaca, New York 14853

J. KIRKBY

CERN, Geneva, Switzerland

M. Abolins, Michigan State University

B. A. Barnett, John Hopkins University

D. M. Binnie, Imperial College

F. Bulos, SLAC

J. Carr, Lawrence Berkeley Laboratory

T. Ferbel, University of Rochester

M. J. Glaubman, Northeastern University

L. Holloway, University of Illinois

J. Huston, University of Rochester

A. S. Kanofsky, Lehigh University

H. J. Lubatti, University of Washington

J. Marriner, Fermilab

R. J. Morrison, U. C. Santa Barbara

A. Odian, SLAC

L. Price, Argonne National Laboratory

R. Ruchti, University of Notre Dame

P. Slattery, University of Rochester

G. Snow, University of Maryland

P. Sokolsky, University of Utah

Y. Suzuki, Osaka University

H. H. Williams, Univ. of Pennsylvania

R. K. Yamamoto, MIT

G. B. Yodh, University of Maryland

### Summary

The 4 $\pi$  Detector Working Group tried to address two major questions:

1. Can general 4 $\pi$  detectors be built for the SSC that will be able to study rare processes at center-of-mass energies of 40 TeV and at luminosities of  $10^{33}$  cm $^{-2}$ sec $^{-1}$ ?
2. What are realistic cost estimates for such detectors?

To try to answer these questions, the group split into three subgroups, each of which worked fairly independently to design a detector. Gary Feldman led the subgroup that designed a non-magnetic detector called D1; Gil Gilchriese led the subgroup that designed a magnetic detector called SCD, which employs conventional technology; and Jasper Kirkby led the subgroup that designed a magnetic detector called SciFiD, which has a non-conventional tracking system.

The general conclusions of these studies were that these types of detectors could be built, would be able to do physics under these conditions, and would each cost between 200 and 300 million dollars.

### The D1 Detector

The D1 Detector<sup>(1)</sup> is a non-magnetic detector which is designed to measure the "partons" which emerge from proton-proton collisions. By "partons" we mean quarks and gluons (which materialize as hadronic jets), electrons, muons, photons, and neutrinos (which are measured by missing transverse momentum). The detector is designed to make these measurements at a luminosity of  $10^{33}$  cm $^{-2}$ sec $^{-1}$  and with a reasonably uniform response over plus or minus five units of rapidity. This rapidity range corresponds to the region in which W bosons are produced at 40 TeV center of mass energies.<sup>(1)</sup> (See Fig. 1.) The first question that one should ask is "Why a non-magnetic detector?" There are several advantages:

1. The tracking will be much simpler since straight lines rather than helices must be fit. This means that a non-magnetic detector can have either a more conservative design (for a fixed number of wires) or a smaller number of wires (for an equal level of conservatism).

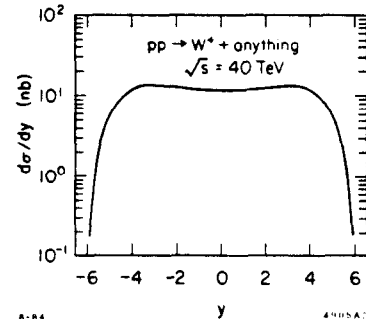


Fig. 1. Rapidity distribution of W bosons produced at 40 TeV center of mass energy. From Ref. 2.

2. The detector can be more compact since magnetic detectors with conventional detectors require a large tracking volume to obtain the necessary resolution.
3. There is no hole in the calorimetry caused by a large coil.
4. The flexibility of not having a coil allows easier coverage of the full rapidity range. The two magnetic detectors described in this report make high-quality measurements in the central rapidity region but have difficulty maintaining the quality of the measurements in the more forward regions.

At the level of measuring partons the principal disadvantage in not having magnetic analysis is that the sign of electrons cannot be determined. However, even in a "non-magnetic" detector, it is necessary to measure the muon momentum (and thus sign) by magnetic analysis. This mitigates the importance of the electron sign measurement. The lack of magnetic analysis both helps and hinders electron identification. On one hand one loses the ability to make energy-momentum comparisons; on the other hand the electron-positron pair from a photon conversion or Dalitz decay stay together and can be distinguished by  $dE/dx$  measurements.

A sketch of the D1 Detector is shown in Fig. 2(a). There are four main systems which we will discuss below in turn.

\* Work supported in part by the Department of Energy, contract DE-AC03-76SF00515.

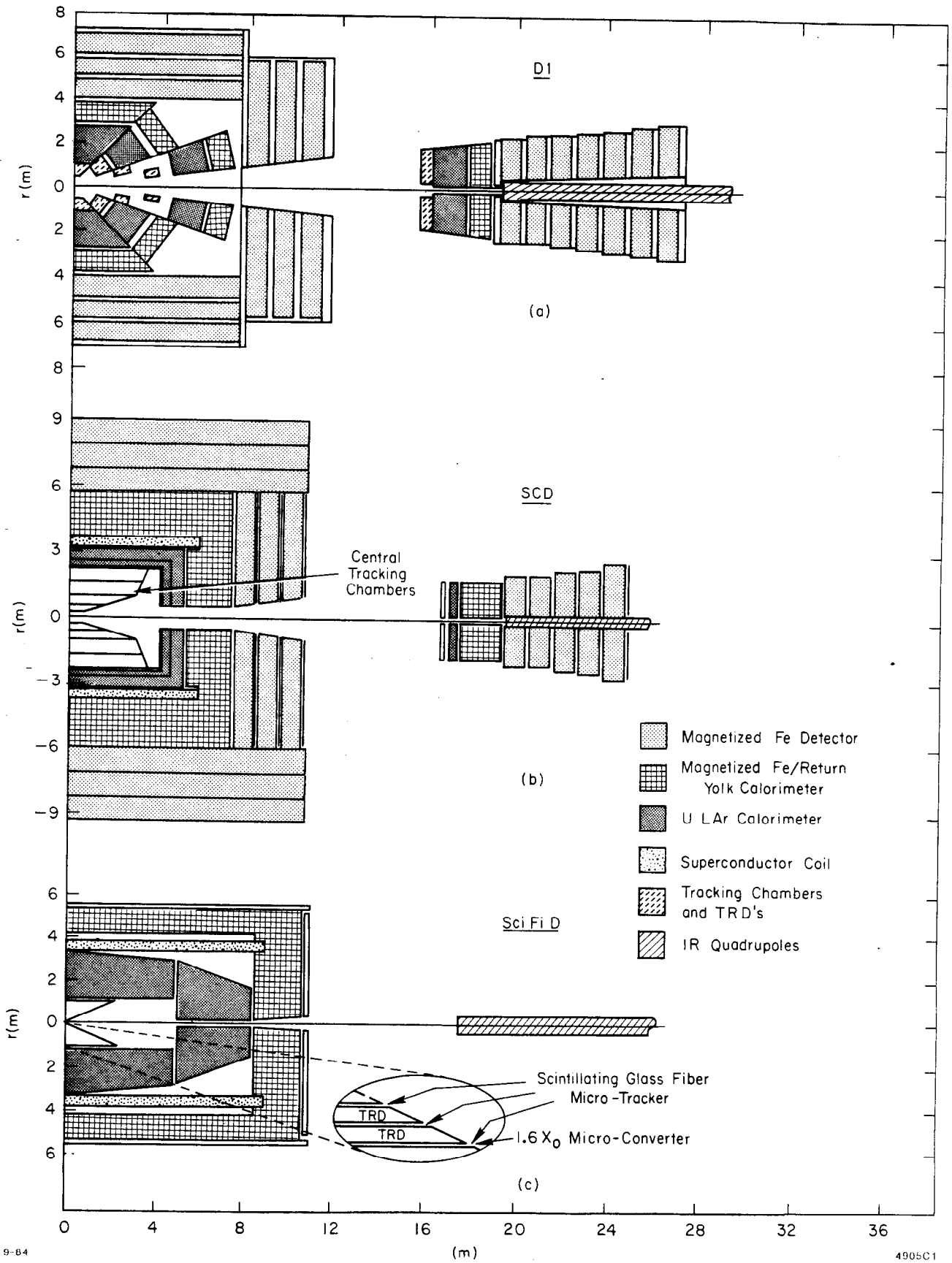


Fig. 2. Schematic drawings of (a) the D1 detector (b) the SCD detector, and (c) the SciFiD detector.

## D1 Tracking System

The goals of the tracking system are

1. to measure multiplicity distributions and jet topologies,
2. to distinguish multiple events from their vertices and determine which tracks belong to each event,
3. to determine which beam crossing each track belongs to by timing,
4. to separate photons and  $\pi^0$ 's from electrons by pointing to the calorimeter, and
5. to distinguish photon conversions by  $dE/dx$  measurements.

Several considerations determine the design of the tracking system. In order to keep the occupancy low it is necessary to use a small wire spacing and to move the detectors farther from the interaction region as rapidity increases. In general one wins in occupancy rate as the inverse square of the wire spacing. One factor comes from the multiplicity of wires and the other factor comes from the reduced drift time. If there is a constant multiplicity per unit rapidity, then in order to keep the occupancy constant with rapidity the detectors should be arranged on a cylinder concentric with the beam line. A strict application of this rule is not practical but the D1 Detector design tries to approximate it.<sup>[1]</sup>

In order to measure the vertices well, the drift direction should be the rapidity direction, rather than the azimuthal direction required in a solenoidal magnetic detector. Figure 3 shows the arrangement of the chambers in a "cobweb" arrangement, which has no cracks pointing to the interaction region. All of the elements of the detector are arranged in eight azimuthal segments. Within each tracking segment there are four drift chamber modules interspersed with four transition radiation detector modules. Each drift chamber module has five staggered layers with 5 mm sense wire spacing. The staggered wires allow the crossing time to be determined with a resolution of about 4 ns. The azimuthal coordinate is measured by charge division with an overall resolution of about 3 mm at the calorimeter face.

The entire detector ( $|\eta| \leq 4.7$ ) requires 184,500 sense wires. The typical occupancy from accidental events is 4% and in the hottest spots it reaches no more than 8% (at  $10^{33} \text{ cm}^{-2} \text{ sec}^{-1}$ ). Although this is a low enough occupancy to allow efficient tracking, it should be remembered that this means there are over 7000 hits in the chambers even for a random trigger.

The rms  $dE/dx$  resolution of about 13% should be good enough to distinguish conversion pairs easily.

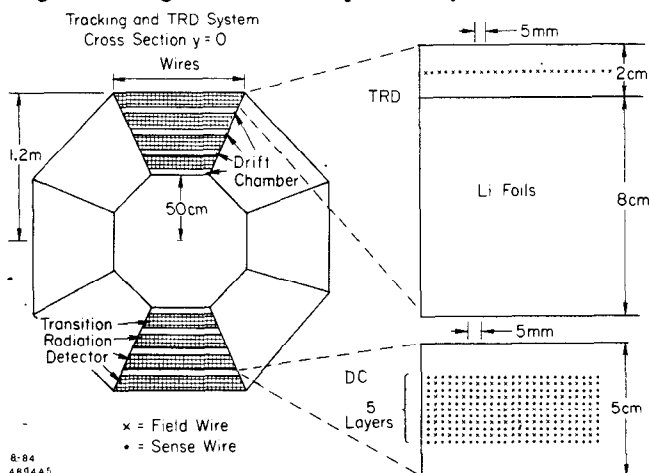


Fig. 3. Details of the D1 tracking and transition radiation systems.

## D1 Transition Radiation Detectors

The goal of the transition radiation detectors<sup>[4]</sup> (TRD's) is to provide an independent hadron/electron rejection factor of 50 beyond the factor of 1000 expected from the calorimeters. The TRD's are effective in the momentum range between 2 and 200 GeV/c. Beyond momenta of 200 GeV/c pions cause a substantial amount of transition radiation; however, the TRD's are still useful for energies above 200 GeV because they can prevent a low momentum hadron from simulating a high energy electron.

The D1 design has four 10-cm thick modules sandwiched radially between the drift chamber modules. (See Fig. 3.) Each module consists of 8 cm of lithium foils and a 2-cm thick xenon drift chamber. The 400 ns drift time of this chamber necessitates the readout of both pads and wires to keep the occupancy rate reasonable. The wire spacing is 5 mm; the pads segmentation is matched to the calorimeter with  $\Delta\eta = \Delta\phi = 0.02$ . There are a total of 36,900 wires and 126,000 pads over the full rapidity range. The occupancies from overlapping events should average 26% for wires and 7% for pads, giving an average 2% occupancy for each wire-pad combination.

A hadron/electron rejection factor of 50 is expected for an electron efficiency of 90%.<sup>[4]</sup> Once efficient, the TRD is a fail-safe device in that high backgrounds make it ineffective, but do not reduce the efficiency for detecting electrons.

## D1 Calorimetry

The goals of calorimetry are

1. to obtain the best possible hadronic energy and angular resolution, and
2. to identify electrons by their transverse and longitudinal shower pattern.

The first goal is necessary because of the difficulty expected in extracting signals for new physics from large backgrounds. In many cases the energy resolution itself is not as critical as the absence of large fluctuations which would give tails to distributions such as those for missing transverse momenta. All three detectors have chosen uranium-liquid argon calorimeters. Uranium was chosen to equalize the response to hadronic and electromagnetic energy, and thus reduce fluctuations;<sup>[5]</sup> liquid argon was chosen because of its stability and radiation hardness.

Electrons can be identified by the pattern of transverse and longitudinal energy deposit with a hadron/electron rejection of about 1000:1.<sup>[6]</sup> At least three longitudinal segments are required to achieve this segmentation.

The design specifications are given in Table II. There are three sections to the calorimeter: an electromagnetic section, a hadronic section, and a catcher section. The electromagnetic section has 30 radiation lengths of fine grained uranium and copper plates to contain and measure accurately the energy and angles of photons and electrons. The use of some copper reduces the cost without greatly affecting the compensation.

The hadronic section is similar but uses thicker plates. The catcher section, however, is made from sandwiches of 5 cm iron plates and wire chambers with pad readouts. The electromagnetic and hadronic sections provide 7.0 nuclear absorption lengths of material and absorb at least 95% of the hadronic energy.

It is important to have a total of around 12 absorption lengths of material to reduce fluctuations due to the leakage of high energy showers from the rear of the calorimeter. However, since the total amount of energy deposited between 7 and 12 absorption lengths is quite small, it is not necessary to have a high quality calorimeter in this region. This is one of the reasons for the use of iron in the catcher section. The other is that the iron is magnetized and forms the first part of the muon identification system.

In this design the transverse segmentation is uniform with towers of size  $\Delta\eta = \Delta\phi = 0.04$ . An alternate design might use  $\Delta\eta = \Delta\phi = 0.03$  segmentation in the electromagnetic section and  $\Delta\eta = \Delta\phi = 0.06$  segmentation in the hadronic and catcher sections, leaving the total number of channels approximately the same. Deciding which scheme is superior will require a more detailed study than we have been able to do so far.

The calorimetry extends over the rapidity range  $|\eta| \leq 5.5$  with coarser transverse segmentation in the region  $4.0 \leq |\eta| \leq 5.5$ . There are a total of 31,500 towers and 157,500 channels. The mass of the liquid argon part of the calorimeter is 1330 tons of which the uranium composes 870 tons. The iron part of the calorimeter has a mass of 1780 tons.

The occupancy from overlapping events is about 14%, but most of the occupied cells will have low energies in them.

#### D1 Muon Identification

The goal of the muon identification system is to identify muons and to measure their momentum over a large rapidity and momentum range. Errors in measuring the muon momenta will be reflected directly in errors in the measurement of missing energy since the calorimeters are insensitive to muons.

The muon identification system consists of 4 ( $|\eta| \leq 3.0$ ) or 8 ( $3.0 \leq |\eta| \leq 4.7$ ) meters of toroidally magnetized iron, the first meter of which is the catcher section of the calorimeter. The muon momentum and position is measured by five sets of chambers, located before, after, and within the iron. Each set of chambers has four layers having a total thickness of 10 cm so that the angle of the muon can be measured at each point. The azimuthal coordinate is measured by charge division. There are also two layers of scintillators to provide a fast trigger.

For lower momenta (below 400 GeV/c in the central region and below 1.6 TeV/c in the forward region) the momentum resolution is determined by multiple scattering in the iron. In these regions the rms fractional resolution is approximately 10% in the central region and 7% in the forward region. For higher momenta the momentum resolution is determined by the chamber resolution and the alignment precision. For a 200  $\mu\text{m}$  resolution per wire and a 100  $\mu\text{m}$  alignment error, the momentum resolution should be about 30% at 2 TeV/c in the central region and at 8 TeV/c in the forward region.

There are 65,400 wires in the system and the total mass of the iron toroids (excluding the catcher section of the calorimeter) is 21,000 tons.

There are 30 nuclear absorption lengths in the central region and 53 in the forward region. Thus, the most important background will be muons from pion and kaon decay at a rate of about  $10^{-3}$ .

#### D1 Trigger

The trigger must select about one in  $10^8$  of the interactions for recording and future analysis. A multi-level trigger is required. The first level will make a decision in about 30 ns using pipelined data from clusters of calorimeter towers and the muon scintillators. Higher trigger levels will use finer and more accurate calorimeter information, muon tracking information, and pulse heights from the TRD pads. Tracking information can probably be used only at the highest level of the trigger which will consist of a large parallel bank of microprocessors analyzing individual events.

#### The SCD Detector

The Super Collider Conventional Detector (SCD) was designed to use a minimum of unconventional technology. It was designed

1. to operate at a luminosity of  $10^{33} \text{ cm}^{-2}\text{sec}^{-1}$ ,
2. to provide excellent tracking in a magnetic field in the rapidity range  $|\eta| \leq 1.5$ ,
3. to have excellent electron identification in the range  $|\eta| \leq 1.5$  with some identification out to  $|\eta| \leq 3.0$ ,
4. to have muon identification for  $|\eta| \leq 4.5$ ,
5. to have good hadron calorimetry for jet studies for  $|\eta| \leq 5.0$  and to measure missing transverse energy, and
6. to contain the option of having precision secondary vertex detection for  $|\eta| \leq 1.5$  at luminosities of  $10^{32} \text{ cm}^{-2}\text{sec}^{-1}$  (or higher if possible).

An overall view of the SCD is given in Fig. 2(b). It is approximately 16 m in diameter and the forward muon detectors extend to  $\pm 26$  m from the interaction point. The interaction region quadrupoles are assumed to be at  $\pm 20$  m from the interaction point. Each section of the detector is discussed below.

#### SCD Silicon Strip Detectors

The operation of central tracking chambers at a luminosity of  $10^{33} \text{ cm}^{-2}\text{sec}^{-1}$  demands fine granularity in order to minimize radiation damage, to reduce excessive rates, and for reasonable pattern recognition. The subject of radiation damage to wire chambers and their rate limitations is discussed in more detail in the report from the Tracking Group.<sup>17</sup> The innermost elements of the central tracking system are two silicon strip detectors each with crossed layers yielding both  $\phi$  and  $z$  coordinate measurements. The inner layer is assumed to be at a radius of 2 cm, have a length of 10 cm and have a strip-to-strip separation of 25  $\mu\text{m}$ . The outer layer might be at a radius of 5 cm, be 20 cm long and have 60  $\mu\text{m}$  strips. The readout electronics is assumed to be integral with or bonded to the silicon in a manner now under development for the Mark II detector at SLC.<sup>18</sup> Although there is some evidence that the silicon strips themselves may survive for more than one year at luminosities of  $10^{33} \text{ cm}^{-2}\text{sec}^{-1}$ , the integrated electronics is presently much more susceptible to radiation damage and would clearly limit the operation of these devices. The assumption here is that intensive study will allow radiation hardened electronics to be used and/or some of the electronics will be located at a greater distance from the interaction point. The maximum usable luminosity is obviously unknown at present but one should note that substantial new physics is, in principle, accessible at  $10^{32} \text{ cm}^{-2}\text{sec}^{-1}$  which appears to be within reach of present hardening techniques.<sup>19</sup>

## SCD Central Wire Chambers

The construction of wire tracking chambers which will survive and produce useful information at a luminosity of  $10^{33} \text{ cm}^{-2} \text{ sec}^{-1}$  at the SSC is one of the most challenging aspects of  $4\pi$  detector design. In the SCD a "brute force" approach is used to solve these problems. The effects of radiation damage are reduced by operating the chambers at a relatively low gain and by having many wires. Occupancy is also reduced by having many wires.

The principle of the mechanical design is discussed in the Tracking Group report.<sup>[7]</sup> The idea is to use modular construction in order to minimize the size of the wire tension support structure and to allow parallel construction of all modules at the same time. Each module would be a self-contained gas tight unit. The wire tension would be supported by inner and outer cylindrical walls constructed of either low-density honeycomb (plastic) and graphite/epoxy or thin aluminum sheets, or low-density foam sandwiched between graphite/epoxy sheets. Such a structure should be able to support the wire tension load with a minimum of material, perhaps 0.7% or less of a radiation length for each module.

In the innermost modules the cell structure probably would be a staggered cell arrangement rather than jet-type cells. In order to minimize cell occupancy the wire spacing in these modules must be as small as possible. The assumption is that the innermost layer has a sense wire to sense wire spacing of 1 mm. Such small wire spacing would almost certainly require a support near the center of each wire which would be built into the module design. The wire spacing would increase somewhat with a radius to about 4 mm at a radius of 1.0 m. Measurements of the z coordinate would be provided by small angle stereo and segmented cathode strips at the inner and outer radii of each module. The strips would be segmented in  $\phi$  as well as in the z coordinate and yield a spatial precision of better than 1 mm for isolated tracks. Each of the two modules contains about 18,000 wires and approximately 6500 cathode strips. This is similar in magnitude to a new drift chamber for the CLEO experiment presently under construction which contains 12,000 wires and 4500 strips.<sup>[10]</sup> The signal density would, however, be about 3 times that in the CLEO design. With considerable effort this signal density might be handled by the conventional means of hybrid or integrated circuit preamplifiers followed by a cable or twisted pair line for each signal. A multiplexed readout scheme using local storage of time and pulse height information would be preferred but would require much more development.

The remainder of the central tracker is contained in two more modules located at radii of 1.0 m to 2.35 m. In each module the outermost 2 cm or so contains three layers of small cells ( $\leq 4$  mm) in order to have low occupancy measurements throughout the chamber. Staggered cells or tiled jet cells would be used in the rest of the area. A serious Monte Carlo simulation is needed to decide which configuration is superior for pattern recognition. In any case the maximum drift time would not exceed 100 ns.

In total the central tracker contains about 130,000 active wires and cathode strips, which is about 8 or more times the number in chambers presently under construction. Parallel construction of the four modules is essential in order to have a reasonable construction schedule. Semi-automated wire stringing techniques would be required to further reduce the construction time. Winding many wires as is done in the construction

of planar chambers may be one way to reduce the construction period. Even without such methods the parallel construction could probably be done within 2-3 years after a final design had been reached.

The momentum resolution of the central tracking chamber is calculated assuming a spatial resolution of 200  $\mu\text{m}$ , 75 coordinates per track and a magnetic field of 1.5 T. The result is  $\partial p/p \approx 3.0 \times 10^{-4} p$  (p in GeV) which is sufficient to determine particle sign at about 1 TeV. Approximately 10 out of the 100 layers would be instrumented for  $dE/dx$  measurements in order to detect overlapping tracks. A summary of the central tracking chamber characteristics is given in Table I.

## SCD Calorimetry

Electromagnetic and hadron calorimeters will be the most crucial elements for any  $4\pi$  detector at the SSC. In the SCD a compromise approach has been taken between having the best possible hadron calorimetry and cost. Uranium-liquid argon (U-LAr) is the preferred method of calorimetry because of its high density and stability. The cost of a complete U-LAr system in a magnetic detector like the SCD would be very large because of the enormous volumes required.

Since electron identification is expected to be very important for the physics to be done at the SSC this is provided by highly segmented U-LAr calorimeter modules which cover the rapidity range  $|\eta| \leq 5.0$ . The calorimeters are  $40 X_0$  deep for normal incidence in order to fully contain multi-TeV electron showers. Each electromagnetic calorimeter is segmented into three elements in depth in order to improve hadron rejection. Naturally a tower structure is used throughout the entire range of rapidity. In the central region,  $|\eta| \leq 1.5$ , a transverse segmentation of  $\Delta\eta = \Delta\phi = 0.02$  is maintained in order to have good electron identification near jets and for jet mass reconstruction. In the larger rapidity regions the granularity varies from  $\Delta\eta = 0.03$  to  $\Delta\eta = 0.10$ . Fine segmentation over the entire rapidity range is, of course, desirable but costly and probably not necessary for new physics which will primarily appear in the central region.

The calorimeter construction is assumed to be similar to the D0 and SLD designs. The uranium plates are 1.6 mm thick ( $0.5 X_0$ ) throughout the electromagnetic calorimeter interspersed with liquid argon gaps (about 1.6 mm) and readout pads (steel, copper or printed circuit boards) on either side of the uranium plates.

Uranium-liquid argon is also used for the first few hadronic absorption lengths for  $|\eta| \leq 3.0$ . These calorimeters would be in the same cryogenic system with the corresponding electromagnetic section and are contained within the magnetic field volume. In the barrel region the hope is to absorb most of a hadronic shower in the U-LAr calorimeters before the tail of the shower passes through the magnet coil and cryostat. In particular one wants enough uranium such that shower maximum occurs about one absorption length before the coil. The total number of absorption lengths before the coil at  $\eta = 0$  is about 5.2, which should be sufficient for this purpose. (There is some disagreement about the depth required for hadronic showers — see the summary of the Calorimetry Group<sup>[11]</sup>). The transverse segmentation is matched to that in the electromagnetic calorimeter section by having one hadronic tower for every four electromagnetic towers. This is again a compromise between

Table I. Tracking Systems

	D1	SCD	SciFiD
Type	Wire chambers	Wire chambers <sup>a</sup>	Scintillating glass optical fibers
Principal coordinate	$z$	$\phi$	$\phi$
Secondary coordinate measurement technique	Charge division	Small angle stereo and cathode strips	Small angle stereo
Radial extent ( $z=0$ )	50 to 100 cm	25 to 235 cm	10 to 100 cm
Rapidity range	0 to 4.7	0 to 1.5 (central) 1.5 to 5.0 (endcap)	0 to 1.5
Cell spacing	5 mm	1 to 4 mm	25 mm
Number of hits per track	20	100 (wires) 6 (strips)	130
Number of dE/dx layers	20	10	none
Number of channels	184.5 k	100 k wires <sup>b</sup> 32 k strips	150 M fibers 38 M cells <sup>c</sup> 920 CCD's
Resolutions: <sup>d</sup>			
principal coordinate	200 $\mu\text{m}$	200 $\mu\text{m}$	10 $\mu\text{m}$
secondary coordinate	1 cm	1 mm	70 $\mu\text{m}/\text{su}$ per layer
track pair	5 mm	1-4 mm	50 $\mu\text{m}$
momentum	none	$3 \cdot 10^{-4} p$	$2.5 \cdot 10^{-4} p \oplus 0.031$
<p><sup>a</sup> Inner silicon strip detectors are omitted from this table.</p> <p><sup>b</sup> There are an additional 30 k channels in the endcap tracking system.</p> <p><sup>c</sup> Cells are defined by the image intensifier resolution.</p> <p><sup>d</sup> Spatial resolutions are per measurement unless stated otherwise.</p>			

cost and the optimum granularity. Hence in the central rapidity region the hadron calorimeter has  $\Delta\eta = \Delta\phi = 0.04$ , with larger values in the smaller-angle region. There is no segmentation in depth.

The magnet return yoke is instrumented as a hadron calorimeter with gas tubes and pad readout. In the barrel region the first meter of iron is segmented into 20 plates each 5 cm thick with tubes and pads between the plates. The remainder of the yoke is made of five 10-cm plates with similar readout. There is no segmentation in depth — each tower sums over the entire 1.5 m of iron. The endcaps are of a similar construction but have an additional 50 cm of iron.

The forward hadron calorimeter has been chosen to be iron-gas tubes although there is some doubt about radiation damage in such devices. There seems to be no compelling reason (except uniformity) to have U-LAR hadron calorimetry in this region but this question needs more quantitative study. The electromagnetic calorimeter in this region is still U-LAR because of possible saturation effects in gas electromagnetic calorimeters at TeV energies and to have some amount of electron identification for dilepton events in this rapidity region. A summary of the calorimetry in SCD appears in Table II.

#### SCD Magnet and Return Yoke

The magnetic field in SCD is provided by an enormous magnet assumed to operate at 1.5 T. This superconducting magnet is about twice as long as the magnet proposed for the SLD detector, slightly larger in radius and with 50% more field. The feasibility of such a large magnet was not investigated in any detail but it seems to be a straightforward extension of current techniques.

The return flux is carried by an iron yoke which also acts as a hadron calorimeter and a muon filter. Approximately 1.5 m of iron is required as a flux return.

#### SCD Muon Detector

Muon detection is straightforward but expensive in SCD. Three sets of magnetized iron toroids are used to detect muons by penetration and to make an additional measurement of their momenta. The latter is particularly important for  $|\eta| > 2$ , where the central tracking chamber has poor resolution, and for muons near or inside jets for all rapidity regions. At least one meter of magnetized iron plus chambers is required to make a  $p_{\perp}$ -selective muon trigger. Penetration through iron alone is insufficient to reduce the single muon trigger rate to a low enough value. More iron is needed to make reasonable momentum measurements. The amount of magnetized iron in SCD is 3 m in the

Table II. Calorimeters

	D1	SCD	SciFiD
Type			
electromagnetic	U-Cu/liquid Argon	U-Cu/liquid Argon	U-Cu/liquid Argon
hadronic	U-Cu/liquid Argon	U-Cu/liquid Argon*	U-Cu/liquid Argon
catcher/flux return	Fe/wire chambers	Fe/wire chambers	Fe/wire chambers
Thickness			
electromagnetic	30 $X_0$ (1.4 $\lambda$ )	40 $X_0$ (1.2 $\lambda$ )	40 $X_0$ (1.5 $\lambda$ )
hadronic	5.6 $\lambda$	4.0 $\lambda$	8.5 to 13 $\lambda$
catcher/flux return	5.0 $\lambda$	9.0 $\lambda$	5 to 8 $\lambda$
Rapidity range	0 to 5.5	0 to 5.0	0 to 5.0
Sampling thickness			
electromagnetic	0.6 $X_0$	0.5 $X_0$	0.5 $X_0$
hadronic	0.03 $\lambda$	0.03 $\lambda$	0.03 $\lambda$
catcher/flux return	0.3 $\lambda$	0.3 $\lambda$	0.3 $\lambda$
Longitudinal segments	5 (3 in EM)	5 (3 in EM)	5 (3 in EM)
Tower size ( $\Delta\eta = \Delta\phi$ )			
electromagnetic	0.04	0.02 to 0.1	0.03
hadronic and catcher	0.04	0.04 to 0.2	0.06
Number of towers			
electromagnetic	31.5 k	45 k	48 k
hadronic and catcher	31.5 k	11 k	12 k
Number of channels	157.5 k	166 k	180 k
Mass			
U-liquid Ar	1330 T	2440 T	2400 T
Fe-gas	1780 T	6900 T	6300 T

\* The forward hadronic calorimeter is constructed from iron-gas tubes sandwiches.

barrel toroids and endcap toroids and 5 m in the forward toroids. More iron would in fact be useful in the barrel and endcap regions in order to measure momenta above 1 TeV but adds tens of millions of dollars to the overall cost. It may be cheaper to improve the muon chamber spatial accuracy rather than add more iron.

In the barrel region the entering muon angle is measured by four layers of chambers just outside the return yoke and by chambers between the meter-thick magnetized slabs. The last set of chambers also includes four layers for a measurement of the exit angle. A single measurement by current division is used per layer in the non-bending direction. The barrel toroids weigh about 23,400 tons and the endcap toroids about 4400 tons. The forward system amounts to 1000 tons. Scintillator is not used as a fast level 0 trigger, but rather the chambers are assumed to fulfill this function. This means that at least some of the chambers must have rather small wire spacing ( $\sim 1$  cm) for speed.

### The SciFiD Detector

This section will describe an unconventional SSC  $4\pi$  detector, shown in Fig. 2(c), which is named SciFiD, an acronym referring to the novel central tracker: Scintillating Fiber Detector.

The primary purpose of the SSC is to expose new particles and new interactions in the 0.5-3 TeV/ $c^2$  mass range. These hard processes will populate the central rapidity region; for example in the decay  $Q \rightarrow Wq$  of a heavy quark of mass 0.5 TeV/ $c^2$ , 60% of the W's are produced in the rapidity range  $-1.5 < \eta < 1.5$  ( $25^\circ < \theta < 155^\circ$ ). The decay products of higher mass objects will be even more centrally produced.

No strong justification is seen for  $\pi/K/p$  identification in a  $4\pi$  detector. The only foreseen application is towards heavy flavor tagging by D and B reconstruction, but even here particle identification is not crucial. This is welcome news experimentally since it is impossible to include broad-band  $\pi/K/p$  identification without severely compromising other parts of the detector.

With these simple observations we can specify the following design criteria for SciFiD:

1. Excellent and uniform detection of all particles in the central rapidity region,  $|\eta| < 1.5$ .
2. Calorimetry and  $\mu$  tagging over almost all of the solid angle ( $|\eta| < 5$ ), in order to provide a hermetic detector for  $\nu$  (or  $\bar{\nu}$ ) identification and to ensure excellent jet efficiency and jet energy resolution. (In order to contain 95% of the energy of a quark or gluon jet at the SSC, it is necessary to integrate over a cone of half opening angle  $\simeq 60^\circ$ .)

3. A final criterion – which is not particularly appropriate in this study but of sufficient importance to mention here – is that the detector design has a built-in flexibility to upgrade after its initial operation. Examples of such flexibility are: making calorimeter pad sizes smaller than the original design specifications and hard wiring them externally, using flexible geometries (not spherical geometry, modular construction, etc.) and leaving space before the calorimeter for future additions.

Guided by these criteria, we will now describe the evolution of SciFiD in order to allow a clearer perspective of the chosen design.

#### SciFiD Design Evolution

The starting point is a uranium-liquid argon calorimeter of sufficient depth to contain TeV hadrons (and therefore multi-TeV jets). Although there is a disagreement between present measurements,<sup>[11]</sup> a 1 TeV hadron shower is approximately 95% contained in 10 to 12  $\lambda$ . The SciFiD uranium calorimeter has a thickness of 10  $\lambda$  at  $\eta = 0$ , increasing to 15  $\lambda$  in the forward direction ( $|\eta| \geq 1.5$ ) to accommodate higher energy jets. Uranium-liquid argon is chosen for the same reasons it was chosen by the D1 and SCD detectors, its equal response to hadronic and electromagnetic energy, its stability, and its radiation hardness.

The inner radius of the calorimeter is influenced several factors. Factors which favor increasing the radius are the need for sufficient separation of particles before reaching the calorimeter and the need for space for tracking, momentum measurement and transition radiation detectors. Factors which favor decreasing the radius are the minimizing of pion and kaon decays and detector cost. The last point is perhaps the most serious constraint. There is a fundamental incompatibility between a deep uranium calorimeter and tracking with conventional drift chambers (which require a radius of 2-2.5 m<sup>[7]</sup>). Our solution is to propose a new device, which we call a "micro-tracker", based on scintillating glass optical fibers.<sup>[12]</sup> This system has the potential of meeting all the criteria necessary for the inner tracker:

1. Precise measurement accuracy.
2. Fine two-hit resolution (to resolve particles in jets and to handle multiple events and multiple  $z$  vertices).
3. Radial compactness due to a high density of hits per unit path length.
4. Radiation hardness (both of the device and the local electronics).
5. Fast response for a high rate capability.
6. Good pattern recognition capability (to minimize the computer time for data reduction).

Next we turn to the issue of a magnetic field: "To  $\vec{B}$  or not to  $\vec{B}$  that is the question." A magnetic field is a vital part of the SciFiD detector because it allows the following advantages:

1. Measurement of electron sign.
2. Improved electron identification for momentum/energy match and separation of converted pairs. (But a loss of identification by  $dE/dx$ .)
3. Improved muon identification by matching momentum measured in the inner and outer detectors. This reduces

the background due to punch-throughs and pion and kaon decays.

4. Measurement of the momentum and sign of all tracks.
5. Independent jet measurements.
6. Extra redundancy for isolating rare signals.
7. Internal cross-check of calorimeter energy measurements.

The type of magnet for the central detector is unquestionably a solenoid — it provides an isotropic  $p_{\perp}$  measurement in the central region and the beam spot can be used as a fast momentum measurement in event reconstruction and in the muon trigger. The solenoid coil is traditionally located between the electromagnetic and hadronic sections of the calorimeter in order to avoid degradation of the electromagnetic energy and position resolution. However, in a hadron collider detector it is better to put the solenoid outside the hadron calorimeter for the following reasons:

1. No deterioration of calorimeter performance with respect to energy resolution, shower spreading, or, especially, hermeticity. The coil and cryostat occupy 50 cm radial space and have a thickness of 0.5  $\lambda$ . Placement directly after the electromagnetic calorimeter corresponds to shower maximum for low-energy hadrons and also leads to a serious loss of calorimeter hermeticity in the forward direction.
2. Reduction of uranium mass and calorimeter cost.
3. Presence of a large  $\int Bdl$  for muon momentum measurement, combined with a thick absorber (calorimeter). Muons can be identified and their momenta obtained directly from impact parameter measurements made with chambers located at the solenoid exit.
4. Simplification of calorimeter cryogenics.
5. A thick and robust cryostat and coil can be used.

The disadvantage is, of course, the increased cost of the magnet. However we consider this to be outweighed by the advantages and locate the SciFiD coil outside the hadron calorimeter. The coil is very large: 3.5 m in mean radius and 18 m long (approximately the same size as three SLD coils connected in series).

The final design consideration concerns the muon system. In order to stop 1 TeV hadrons we need 15  $\lambda$  at  $\theta = 90^{\circ}$ . Therefore the combination of the uranium calorimeter and the magnet return yoke provides sufficient absorber for muon detection. In addition, there are three independent measurements of the muon momentum: the central tracker, chambers at the solenoid exit and finally the magnetized iron yoke. The large superconducting coil has eliminated the need for an external system of magnetized toroids.

#### SciFiD Hadron calorimetry

The calorimetry system is summarized in Table II. Here we will make a few additional comments. It is extremely important to have a hermetic detector. This will provide sensitivity to  $\nu$  production at large  $p_{\perp}$  and also to supersymmetric particles, whose only signature is the production of the neutrino-like  $\tilde{\eta}$ . The influence on the design of SciFiD is as follows:

1. Complete calorimeter coverage to within 15 mr of the beam axis.
2. Deep calorimetry (15-23  $\lambda$ , of which the first two-thirds is uranium).



3. Good jet energy resolution and approximately equal  $e$  and  $\pi$  response.
4. Non-projective tower geometry.
5. Muon tagging over the entire solid angle (to veto heavy quark semileptonic decays in a  $\tilde{\gamma}$  search).

Studies indicate that the tails of missing  $p_{\perp}$  distributions are strongly affected by projective dead regions of the calorimeter,<sup>[11]</sup> e.g., a calorimeter with a total of around 5% azimuthal cracks (either massless or massive) will have instrumental missing  $p_{\perp}$  tails dominating over the natural limit set by  $\nu$  production from heavy flavor decays and  $\pi/K$  decays-in-flight. Given the considerable weight of the calorimeters, it is extremely difficult to achieve even a 5% figure for support structures. The solution is to incline the cracks by a large angle of about  $10^{\circ}$  relative to a radially-projective geometry.

The optimum transverse granularity is not well-determined. The argument for going to finer granularity is to improve the mass resolution of high  $p_{\perp}$  particles which decay to several jets, e.g., the reconstruction of  $W$ 's produced in the decays of very heavy ( $\sim 1 \text{ TeV}/c^2$ ) quarks,  $Q \rightarrow Wq$ . In such cases, the dominant influence on the mass resolution is the uncertainty of jet angles. This case was studied and a continual improvement was found as the hadron cell granularity was reduced from  $\Delta\phi = \Delta\eta = 0.1$  to  $0.01$ .<sup>[12]</sup> However, it may be possible to obtain good performance with somewhat coarser cells combined with a jet angle measurement using magnetic analysis of the charged tracks. We adopt this as a plausible solution and have hadronic cells of size  $\Delta\phi = \Delta\eta = 0.06$ . This implies a physical cell size at  $\theta = 90^{\circ}$  of  $6 \times 6 \text{ cm}^2$  at the calorimeter entrance and  $19 \times 19 \text{ cm}^2$  at the exit. Although these dimensions may seem rather narrow compared with the hadronic shower size (95% containment  $\simeq 1\lambda \simeq 20 \text{ cm}$  in U-LAr<sup>[11]</sup>) there is a dense core early in the shower development and our matching to hadronic shower size is reasonable.

### SciFiD Electromagnetic Calorimetry

In order to optimize the analysis of electrons, we employ a very fine transverse granularity in the electromagnetic calorimeter. Each cell subtends a solid angle of about 1 mstr ( $\Delta\phi = \Delta\eta = 0.03$ ) which is equal to the particle density within the "clumps" found in TeV jets at the SSC. A quantitative study shows that this granularity gives good performance for electron identification and measurement with regard to the following:<sup>[11]</sup>

1. Low rate of  $\pi^{\pm}/\gamma$  overlaps and low distortion of transverse position measurement (by energy sharing). Accurate shower position measurements can reduce uncorrelated  $\pi^{\pm}/\gamma$  overlaps by  $10^2$ .
2. Good electron detection efficiency and measurement accuracy due to a low overlap of extra particles.

This granularity is, however, insufficient for high  $p_{\perp}$   $\pi^0/\gamma$  separation. We propose to handle this important measurement in a novel "macro-converter", discussed in the next section.

The cells are deep ( $40 X_0$ ) and, in order to help discriminate against hadrons, are sampled longitudinally in three sections:

- 1) 0-5  $X_0$  : early shower development
- 2) 5-30  $X_0$  : remainder of  $\sim 1 \text{ TeV}$  electromagnetic shower
- 3) 30-40  $X_0$  : fine-grained electromagnetic energy back-catcher to identify penetrating hadrons

### SciFiD Tracking

The micro-tracking system is the key component of the detector; it allows a deep ( $10\text{-}15 \lambda$ ) uranium calorimeter to be built while introducing remarkable performance in tracking and momentum measurement.

We describe the system in detail elsewhere<sup>[13]</sup> and so provide here only a brief summary. Based on the pioneering measurements of Ruchti *et al.*<sup>[14]</sup> we have designed a chamber built from scintillating glass optical fibers of  $25 \mu\text{m}$  diameter. The chamber is built from several "superlayers" of fibers arranged in concentric cylinders. A superlayer consists of four layers, each 2 mm thick, made from coherent arrays of  $\text{Ce}_2\text{O}_3$  glass fibers oriented in the directions  $z$ - $u$ - $v$ - $z$ . The  $u$  and  $v$  fibers form a narrow angle stereo of  $\pm 50 \text{ mr}$  with respect to the  $z$  fibers, which lie parallel to the beam axis. The perpendicular material in each superlayer is  $0.08 X_0$ . The full tracking system comprises:

1. Three superlayers centered on radii of 30, 60, and 90 cm.
2. A 2 mm deep layer of  $z$  fibers at a radius of 10 cm to improve the measurement precision of impact parameters due to secondary decay vertices.

In addition there is a "micro-converter" superlayer located at the entrance of the calorimeter. This employs scintillating fibers made from heavy glass ( $1 X_0 = 1.5 \text{ cm}$ ) of thickness  $1.6 X_0$  ( $z$ ) followed by  $.13 X_0$  ( $u$ ) and  $.13 X_0$  ( $v$ ). The device separates  $\pi^0$ 's from single  $\gamma$ 's up to  $p_{\perp} = 2 \text{ TeV}$ , conservatively assuming a  $150 \mu\text{m}$  two-shower resolution. The  $\pi^0$  detection efficiency is about 50%. Therefore at high  $p_{\perp}$ , where  $\gamma/\pi^0 \sim 1$ , SciFiD has a unique ability to measure single  $\gamma$ 's. The micro-converter layer can also be used to reduce substantially the  $\pi^{\pm}/\gamma$  overlap background for electron measurements, by requiring the electron track to shower (indicated by an increase in the hit density along the track).

The fibers are read out via an image intensifier system onto CCD's. Each  $1 \text{ cm}^2$  of fiber bundle from the chamber is treated as a distinct channel consisting, in order, of the following components:

1. A low gain ( $\sim 100$ ) photodiode system of one or perhaps two stages directly coupled to the chamber. These devices have a blue-sensitive photocathode and a fast green/yellow  $\rightarrow$  red output phosphor. Amplification is provided simply by acceleration of the photoelectrons to about 10 keV between the photocathode and phosphor.
2. A 30 m long coherent bundle of (radiation-hard)  $\text{Ce}_2\text{O}_3$  glass. This provides about 200 ns delay while a primary trigger decision is being made. Light generated in this glass is removed by a suitable filter at the exit of the bundle.
3. A higher-gain ( $\sim 10^3$ ) image intensifier with a gatatable micro-channel plate. The output is coupled to a CCD with pixel size of about  $20 \times 20 \mu\text{m}^2$ . The CCD is continually fast-cleared ( $\tau_{\text{clear}} \simeq 1 \mu\text{s}$ ) until an event of interest is recorded, after which the CCD is read. At present the maximum rate of reading a CCD is about 100 Hz; it may be necessary to increase this to about 1 kHz for our application.

The potential performance of this system as indicated in Table I, is remarkable. If we assume a reasonable factor of two

extrapolation from present measurements to 5 hits/mm, we expect 130 hits per track provided by the three superlayers and inner vertex layer. The pattern recognition capabilities are much superior to drift chambers; each superlayer measures a track vector with a precision  $\sigma_{xy} \simeq 2.2 \mu\text{m}$ ,  $\sigma_{rz} \simeq 70 \mu\text{m}$ ,  $\sigma_\phi \simeq 0.5 \text{ mr}$ , and  $\sigma_\theta \simeq 40 \text{ mr}$ . In addition, by computing the impact parameter with the origin, a track stub in a superlayer has a momentum measurement accuracy of 0.8%, 0.4%, and 0.3% for the superlayers at 30 cm, 60 cm, and 90 cm radius, respectively. These characteristics will allow excellent matching between superlayers and also early identification of the uninteresting but numerous low momentum tracks. After associating the three superlayers, the momentum measurement precision is  $\sigma_p/p = \{[2.5 \times 10^{-4} p(\text{GeV}/c)]^2 + 0.031^2\}^{1/2}$ .

The device has extremely high granularity and can handle the high rates and jet topologies at the SSC. Despite this large granularity, the electronics has built-in multiplexing; there are only about 2 K discrete channels (image intensifier/CCD units), each reading out about  $10^5$  fibers.

Finally it is possible that the  $\text{Ce}_2\text{O}_3$  glass fibers will be able to withstand the high radiation environment of the SSC (about  $5 \times 10^5$  rads per operational year at a radius of 10 cm). This glass was actually developed by the U.S. Navy for its resistance to the radiation environment of nuclear reactors. Doses of about  $10^6$  rads have been delivered to small samples under severe conditions, i.e. in a few seconds, and they have visually recovered in several days. The local image intensification system also has good resistance to radiation.

#### SciFiD Electron Identification

Electrons are identified and measured by a combination of electromagnetic calorimetry, magnetic tracking of charged particles and transition radiation detectors.

The material in the body of the chamber ( $0.18 X_0$ ) generates two problems for electron studies:  $\gamma$  conversions and electron bremsstrahlung, which will spoil the momentum/calorimeter energy match. However, neither effect is overwhelming. In the case of  $\gamma$  conversions, they must occur in the region of the first few hits of a normal track, i.e. within about 0.5 mm or  $0.005 X_0$  of the first fiber layer. In such cases, the superb granularity of the chamber will identify almost all conversions (and certainly reduce them below the  $\pi^0$  Dalitz background rate). The effect of electron bremsstrahlung is to degrade the measured momentum of electrons. However, the same calorimeter cell essentially always sees both the electron and photon and therefore measures the true initial energy. The effect is accommodated by simply widening the allowed range of momentum-to-energy matching.

The transition radiation detectors<sup>(1)</sup> are made from six polypropylene radiator/Xe detector modules, each 10 cm deep. The detectors have wires (which are not read out) and pads which match the electromagnetic calorimeter cells. There are 21 K pads per module; each pad must be individually read out because the extended interaction vertex in  $z$  precludes a unique projective geometry. (Individual readout is also useful to allow truncation before computing the track pulse height.) The system provides about  $3 \times 10^{-3} \pi/e$  rejection below 150 GeV (and above that separates pions from kaons and protons up to about 1 TeV).

#### SciFiD Muon Detection

Muons are identified as stiff tracks which penetrate 15–23  $\lambda$  material. They are measured with a system of chambers which provide track vectors at the exit of the solenoid and at the exit of the magnet flux return. A system of scintillation counters on the outside of the detector is used as a fast first level trigger. Subsequent triggers involve measurements of muon momentum by computation of impact parameter at the beam ( $\delta_{xy} \simeq 7 \mu\text{m}$ ) using either the chamber at the solenoid exit or the outermost chambers. In the latter case, although there is no net magnetic deflection the multiple Coulomb scattering angle of  $.25/p(\text{GeV})$  radians can usefully distinguish between hard and soft muons.

An important characteristic of SciFiD is that the muon momentum is measured three times with a comparable accuracy and so there is excellent rejection of false or badly-measured muons. The muon chambers must have relative systematic alignment errors  $\leq 50 \mu\text{m}$  in order to ensure that measurement errors at 1 TeV do not dominate over the multiple Coulomb scattering errors. The system has excellent performance, measuring  $\mu$  momentum to about 20% at 1 TeV.

#### SciFiD Trigger and Computers

The conceptual scheme for the trigger is as follows:<sup>(11)</sup>

1. Simple dead-timeless triggers from each subsystem are formed rapidly ( $\sim 200 \text{ ns}$ ) and are fanned-in to accept about 0.1% of the  $10^8 \text{ Hz}$  raw event rate. These include calorimeter  $E_\perp$  and missing  $p_\perp$  sums, and muon and electron triggers. This trigger allows data to be transferred from temporary storage devices (such as shift registers) into memory or, in the case of the micro-tracker, onto CCD's.
2. More restrictive levels of hardware triggers, which take correspondingly longer to form, are applied until the event rate is about 1 kHz. No advantage is foreseen in any hardware trigger which uses information from the central tracker.
3. At this stage the whole event is processed by an array of about 1000 parallel processors each taking an average of about 1 s per event. The event is sent through a software filter at various stages during this processing which applies cuts to exclude all events other than those of interest. The final events, which are fully processed, are written on an output device such as tape. By fiat the output event rate is about 1 Hz.

All this sequence occurs locally, near the experiment; the only data to be transported to outside computers are processed data summary tapes. In this way the software is placed at the same priority as the hardware during the construction of the detector. If the software has errors it is just the same as if, for example, there is a bad gas mixture in the muon chambers — the experiment is not taking data. This situation will cause a little lost data at the beginning but ultimately will result in a much more efficient operation and production of physics results. It also leaves external computers uncongested for physics and Monte Carlo analyses rather than being saturated with data reduction. But most important, it will allow for the on-line implementation of a flexible evolving trigger as the luminosity of the SSC improves.

Table III. Cost Estimates (M\$)

	D1	SCD	SciFiD
Tracking system	<b>27.0</b>	<b>28.8</b>	<b>26</b>
mechanical costs	18.5	11.6	10
electronics costs	18.5	17.2	16
Transition radiation detectors	<b>25.6</b>	—	<b>15</b>
mechanical costs	9.2	—	2
electronics costs	16.4	—	13
U-liquid argon calorimeters	<b>39.5</b>	<b>81.0</b>	<b>68</b>
mechanical costs	33.2	73.7	60
electronics costs	6.3	7.3	8
Iron-gas calorimeters	<b>17.0</b>	<b>21.4</b>	<b>14</b>
mechanical costs	15.4	20.4	13
electronics costs	1.6	1.0	1
Superconducting coil	—	<b>19.0</b>	<b>31</b>
Muon detection system	<b>35.3</b>	<b>49.5</b>	<b>16</b>
mechanical costs	28.8	41.5	8
electronics costs	6.5	8.0	8
Trigger and data acquisition	<b>9.9</b>	<b>10.0</b>	<b>10</b>
Totals (before contingency)	<b>164.3</b>	<b>209.7</b>	<b>180</b>
mechanical total	105.1	166.2	124
electronics total	59.2	43.5	56
Contingency (25%)	<b>41.1</b>	<b>52.4</b>	<b>45</b>
Total*	<b>205.4</b>	<b>262.1</b>	<b>225</b>

\* Offline computing costs have not been included in this table. The Computing Working Group estimated that these costs would be about 40 M\$ for a magnetic detector. They should be considerably less for a non-magnetic detector.

### Cost Estimates and Conclusions

All of detector cost estimates were made using a common set of guidelines that are discussed elsewhere in these Proceedings.<sup>[16]</sup> These guidelines were derived from actual or budgeted costs for large detectors which have been or are currently being built. Except for electronics costs, no allowance was made for economies of scale. A summary of these estimates are shown in Table III. A rather arbitrary contingency of 25% has been included, but no explicit budget has been specified for offline computing. The Computing Working Group has estimated that offline computing could cost as much as 40 million dollars for magnetic detectors.<sup>[17]</sup> The overall conclusion from Table III is that these detectors will cost between 200 and 300 million dollars.

It is, of course, possible to reduce the cost of these detectors by making some sacrifices in the detector performance. One explicit exercise was done for the SCD detector and is shown in Table IV. Clearly the cost of the SCD could also be increased with the result of having better detector performance by, for example, adding more iron for muon momentum measurement or by increasing the amount of uranium-liquid argon calorimetry. These studies emphasize that more study is needed of the physics requirements of 4 $\pi$  detectors.

Table IV. Possible SCD Cost Savings

	Cost Saving (M\$)
Reduce the radius of the central tracker to 2 m	0.0
Electromagnetic calorimeter is also reduced in size	2.8
Replace U-LAr hadron calorimeter with Fe-gas	57.9
A smaller magnet coil is needed	7.3
Use less iron for muon identification	13.4
Total Saved	81.4

The costs of these detectors are driven by three factors: (1) the high energy of the SSC, (2) the complexity and density of SSC events, and (3) the high luminosity expected. Reducing the luminosity of the SSC to  $10^{32}$  cm<sup>-2</sup>sec<sup>-1</sup> would decrease the costs of the detectors somewhat, but the savings would probably not be major, because the detector sizes and granularities are driven largely by the energy and complexity of the events.

We anticipate that there will be two general  $4\pi$  detectors at the SSC. One such detector is insufficient because there is a need to cross-check results and to exploit different techniques. On the other hand, the enormous cost, the large number of physicists needed to build and maintain these detectors, and the desire to avoid excessive duplication will probably argue effectively against having more than two such detectors. Thus, a reasonable SSC detector budget would be 500 M\$ plus the cost of the specialized detectors which would go into the other interaction regions.

Finally, we note that the construction time for these detectors is certainly not less than the construction time of the SSC, and is probably longer. (For example, the LEP detectors are requiring eight to nine years from inception to completion.) Thus, it is necessary that a vigorous detector research and development program should be pursued in parallel with the accelerator research and development. The needs for detector research and development can be clearly defined now, without the traditional requirement of a specific experiment. For example, more work is needed on new calorimeter absorber/sampler combinations with  $e/\pi$  response  $\approx 1$ , radiation-hard electronics, and micro-tracking devices. More studies are needed on the requirements for reasonable pattern recognition and track finding, on needed calorimeter granularities, and on triggering capabilities. If we start now, there is a reasonable chance that these detectors can be built and will work.

#### References

1. The name obviously implies that this is a logical extension of the proposed D0 Detector for the Tevatron I Collider. See B. Pifer *et al.*, D0 Design Report, November 1983, Fermilab internal report.
2. E. Eichten, I. Hinchliffe, K. Lane, and C. Quigg, Fermilab report FERMILAB-Pub-84/17-T (1984).
3. There is a possible problem with this design in that the side-splash from the calorimeters may have a detrimental effect on the tracking. More study is needed of this issue.

4. Report of the Electron Identification Working Group, these Proceedings.
5. Recent Monte Carlo calculations suggest that other combinations of absorbers and samplers may be capable of giving an approximately equal response for electrons and hadrons (see the report of the Calorimetry Working Group in these proceedings). The technique is to suppress the electron response by exploiting the transition effect occurring between two materials of different critical energy.
6. R. Engelmann *et al.*, *Nucl. Instrum. Methods* **216**, 45 (1983).
7. G. Hanson *et al.*, "Charged Particle Tracking and Vertex Detection Group Summary Report", these proceedings.
8. S. Parker and J. T. Walker, Physics at the Superconducting Super Collider Summary Report, p. 187 (Fermilab, 1984).
9. See M. Gilchriese, "Radiation Damage and Rate Limitations in Tracking Devices," these Proceedings.
10. CLEO II Proposal, CLNS 84/609, Cornell University Report
11. Report of the Calorimetry Working Group, these Proceedings.
12. D. Binney, J. Kirkby, and R. Ruchti, paper contributed to these Proceedings.
13. J. Hauptman *et al.*, paper contributed to these Proceedings.
14. R. Ruchti *et al.*, paper contributed to these Proceedings.
15. For more details see the reports of the Calorimetry, Electron Identification, and Muon Identification Working Groups in these Proceedings.
16. M. Gilchriese, Detector and Experimental Summary, these Proceedings.
17. Report of the Computing Working Group, these Proceedings.